SAND80-8231
Unlimited Release

Fundamental Combustion and Diagnostics Research at Sandia

D. L. Hartley, M. A. Gusinow

Sandia Laboratories
energy report

SF 2900 Q(8)(3-74)

Issued by Sandia Laboratories, operated for the United States Department of Energy by Sandia Corporation.

NOTICE

This report was prepared as an account of work sponsored by the United States Government. Neither the United States nor the United States Department of Energy, nor any of their employees, nor any of their contractors, subcontractors, or their employees, makes any warranty, express or implied, or assumes any legal liability or responsibility for the accuracy, completeness or usefulness of any information, apparatus, product or process disclosed, or represents that its use would not infringe privately owned rights.

SAND80-8231
Unlimited Release
Printed September 1980

Progress Report

FUNDAMENTAL COMBUSTION AND DIAGNOSTICS RESEARCH AT SANDIA

April - June 1980

Submitted to: Dr. O. W. Adams
Fundamental Interactions Branch
Division of Chemical Sciences
Office of Basic Energy Sciences
Department of Energy
Washington, D. C. 20545

From: Dr. D. L. Hartley, Manager
Combustion Sciences Department
Sandia Laboratories
Livermore, CA 94550

Edited by: Dr. M. A. Gusinow
Combustion Physics Division
Sandia Laboratories
Livermore, CA 94550

FUNDAMENTAL COMBUSTION AND DIAGNOSTICS RESEARCH AT SANDIA

ABSTRACT

The combustion research at Sandia Laboratories sponsored by the Office of Basic Energy Sciences emphasizes basic research into fundamental problems associated with combustion. Special emphasis is placed on the development and application of advanced research methods. The overall program addresses: (1) detailed chemistry of combustion, (2) fundamental processes associated with laminar and turbulent flames, (3) development of research techniques specifically applicable to combustion environments, and (4) operation of the user-oriented Combustion Research Facility.

Attached are status reports on the research sponsored by OBES. The first section contains activities in Combustion Research, the second section contains activities in Molecular Physics and Spectroscopy, and the third section contains activities in Diagnostics Research. The results reported in these three sections are either completed or at an advanced stage. The work presented in the sections entitled "Work in Progress" represents research in its initial stages. Status of the CRF construction and operation are reported elsewhere.

TABLE OF CONTENTS

Page

COMBUSTION RESEARCH

Chemi-luminescence in C_2H_2-O_2 Reactions 11

High-Pressure Soot Formation 13

FTIR Measurement in a Sooting Flame 14

Laser Absorption and Mass Spectroscopy of the OH Radical 15

The Role of the OH Radical in Catalytic Combustion 16

Ammonia/Oxygen Flame Studies 16

Model for Diffusion-Controlled Reduction of Nitric Oxide by Ammonia 19

Confined Axisymmetric Turbulent Jet 20

Turbulent Diffusion Flame Facility (TDFF) 21

Turbulent Reacting Flow Studies 22

MOLECULAR PHYSICS AND SPECTROSCOPY

Observation of an Optical Stark Effect on Vibrational and Rotational Transitions 22

Kinetics of Soot Precursers by XUV Spectroscopy 25

High Temperature Raman Measurements of CO_2 and H_2O 25

On Correlation Functions and Normal Modes 27

Page

DIAGNOSTICS RESEARCH

Two-Line Laser Excited Fluorescence Temperature Measurement 28

Scattered Light - Free Combustion Kinetics 30

PRESENTATIONS 32

PUBLICATIONS 33

COMBUSTION RESEARCH

The studies reported in this section emphasize the fluid mechanics of reacting flows, chemistry associated with flames, and sooting properties of specific combustion environments.

Chemi-luminescence in C_2H_2-O_2 Reactions - M. A. Gusinow

The chemical reaction of C_2H_2 and O_2 is accompanied by both chemi-ionization and chemi-luminescence. The emitted radiation comes from a variety of sources and in general displays different characteristics. In the work to be reported, a mixture of C_2H_2 and O_2 was ignited by a spark and the resulting time varying emission from C_2^*, CH*, and continuum was recorded. (The electron density was monitored by recording the transmission of microwaves (8.5 GHz) through the cell.) Figure 1 represents oscilloscope traces of the transmitted microwaves, CH*, and continuum emission as a function of time for a stoichiometric mixture of C_2H_2 and O_2 (the instrumental dispersion was 11 Å/mm). The C_2^* emission is essentially identical to that of CH*. The continuum was bright and appeared to be centered at approximately 4500 Å. It is important to note that the continuum had the appearance of a continuous spectra at the instrumental resolution of the present experiment. There is evidence from other laboratories that at higher resolution this may in fact be very finely banded. The continuum is thought to be due to

$$CO + O \rightarrow CO_2 + h\nu \qquad (1)$$

There are several interesting features to be noted in Fig. 1: (1) the continuum emission occurs essentially after the CH* and C_2^* radiation, (2) the CH* emission occurs during the buildup to the peak chemi-ionization, and (3) the continuum has a relatively long-lived character which implies either a slow reaction rate of Eq. 1 at the temperatures involved (the temperature has not been measured) and/or a net production of the reactants in Eq. 1. Figure 2 represents the total time-integrated light at three different spectral regions. The 4319 Å (1.65 Å bandpass) continuum was chosen rather than the 4500 Å (they are equivalent) because the spectral response of the system is the same at 4319 Å and 4314 Å and hence the two emissions can be directly compared. The most interesting feature of Fig. 2 is the essential pressure independence of the C_2^* and CH* integrated emissions. It is tempting to argue that this must be due to quenching of the excited states at higher pressures, but it seems very unlikely that both CH* and C_2^* would be quenched to the extent that both curves are flat. The monotonic rise of integrated continuum emission with pressure (implying increased CO_2 production) is exactly the type of behavior one would anticipate <u>a priori</u> (although not necessarily the particular nonlinear behavior).

Experiments are continuing to study the behavior of this system at different equivalence ratios ultimately comparing the results to modeling efforts now underway.

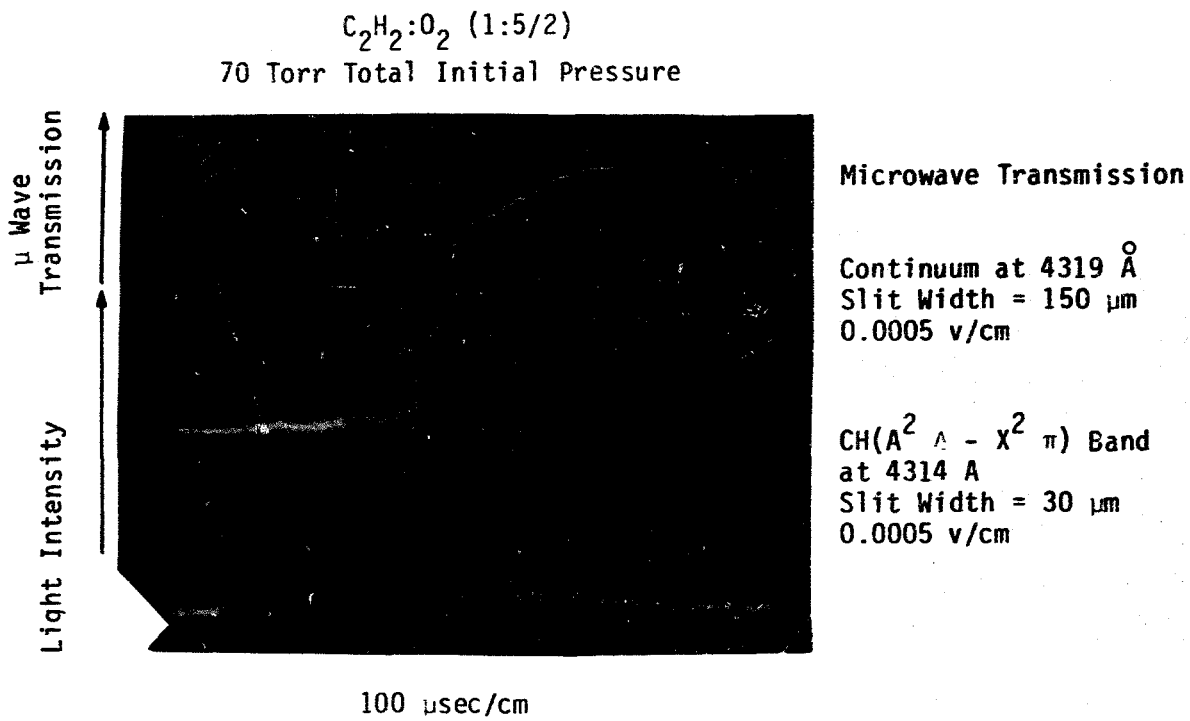

Figure 1: The oscilloscope traces shown are the microwave transmission through the cell, the continuum emission at 4319 Å, and the CH* emission at 4314 Å. These data were taken using a stoichiometric mixture of C_2H_2 and O_2 at 70 torr total initial pressure.

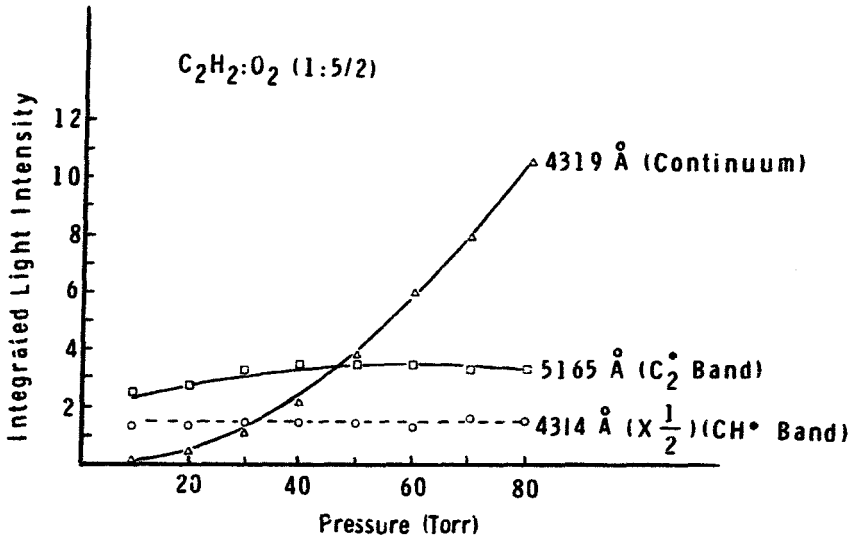

Figure 2: The time-integrated light intensities from three spectral regions are plotted as a function of initial pressure for a stoichiometric C_2H_2-O_2 mixture.

High-Pressure Soot Formation - T. M. Dyer/W. L. Flower

Experiments to characterize and measure soot particulate formation processes are being conducted in a constant-volume combustion bomb. The objective of this work is to provide insight into the origins of soot and its behavior in internal-combustion engines. An important aspect of this work has been the development of an optical pyrometer to simultaneously measure the time- and space-resolved soot volume fraction and temperature of the burned gas.

The current working hypothesis is that while soot formation does depend on equivalence ratio, tne formation is more fundamentally related to the temperature of the burned gas. The burned gas temperature is coupled to equivalence ratio, but it is also strongly dependent on the concentration of diluent in the oxidizer. Therefore, it is possible to test the hypothesis by holding the equivalence ratio fixed and observing variations in soot formation as N_2 diluent and thus flame temperature is varied. In Fig. 3, adiabatic flame temperatures calculated for equilibrium conditions are plotted as a function of equivalence ratio for various diluent concentrations in the oxidizer. The negative slope of these curves results from the fact that excess fuel, beyond the chemically correct point, acts as a diluent to cool the burned gas. Superimposed on these curves is the threshold for soot formation observed in tests in the constant-volume combustion bomb. The low temperature region below the line yields soot and the high temperature region above the line is nonsooting. Increasing quantities of soot are formed at conditions far below the line. The threshold is slowly varying with ϕ and is thus consistent with the hypothesis that soot formation is more directly related to the flame temperature rather than the

equivalence ratio. Such an observation has important implications when attempting to understand the sooting tendency of practical burners as initial conditions are varied. For example, exhaust gas recirculation lowers the burn temperature and hence may be expected to increase soot formation. Conversely, increasing the reactant preheat increases the burn temperature and thus reduces soot production. The fundamental dependence of soot generation on temperature along with the observed pressure dependence provides substantial guidance toward identifying operating regimes which minimize in-situ particulate formation.

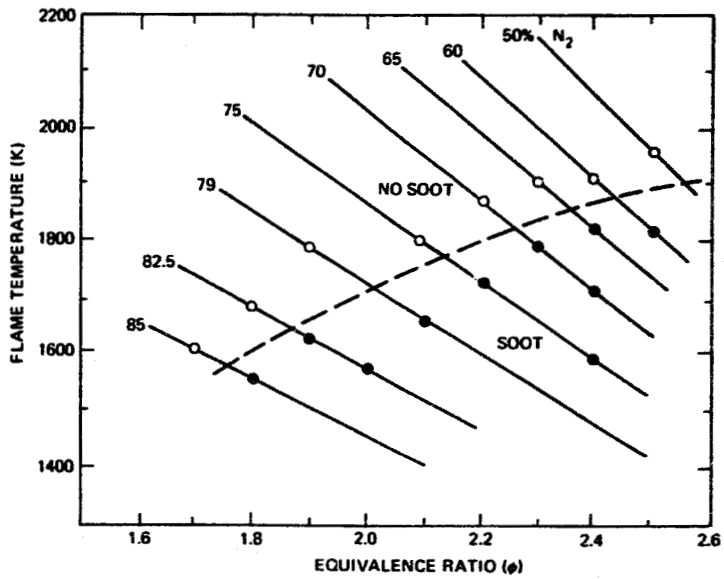

Figure 3: Calculated adiabatic flame temperatures change dramatically as the diluent concentration varies for a given equivalence ratio. Percent N_2 in various O_2/N_2 blends are indicated on the parametric curves. The dashed curve indicates the experimental threshold for soot formation dividing regions yielding soot (·) from nonsooting regions (o).

FTIR Measurement in a Sooting Flame - D. A. Stephenson/D. K. Ottesen

A joint project to determine the feasibility of using Fourier Transform Infrared (FTIR) spectroscopy to measure hydrocarbons in flames, particularly those which might be soot precursors, has been initiated. To this end, a simple kerosene lantern flame has been set up in front of the FTIR spectrometer and the absorption spectrum measured as a function of height above the wick. Figure 4 shows the absorption in the region of the C-H stretch. In rough terms, the hydrocarbon concentration was greatest near the wick and decreased as the measurement region was moved up in the flame. There is some indication of a change in the shape of the C-H band as a function of position, but this must be viewed with caution because of the irreproducible nature of the kerosene flame.

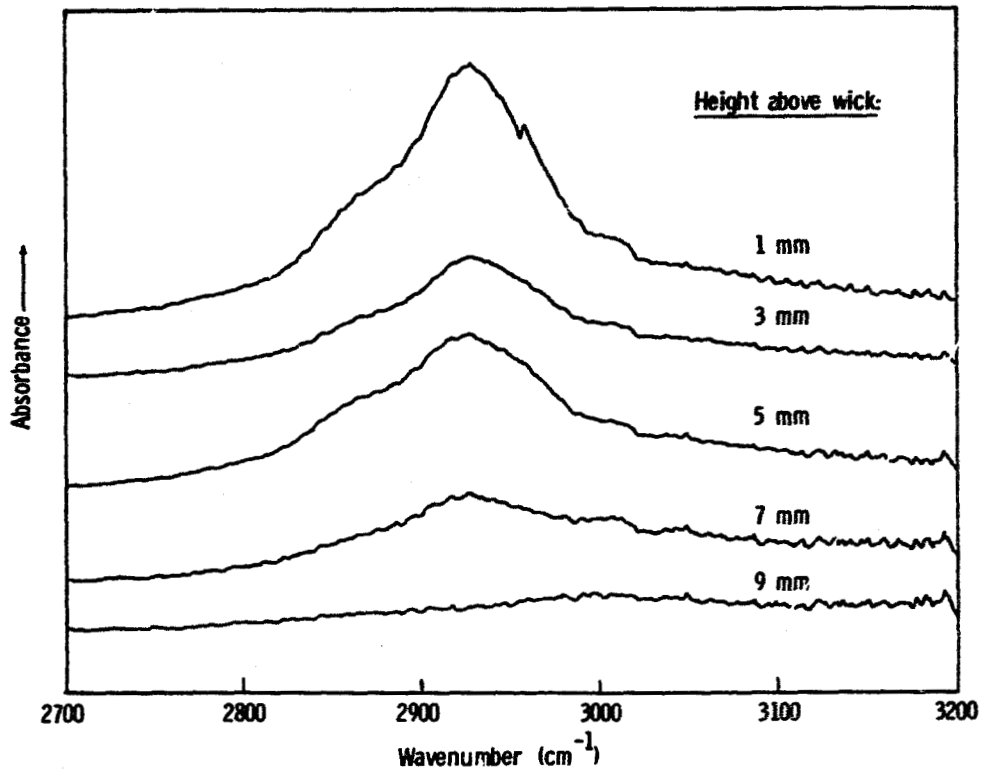

Figure 4: The absorbance of a kerosene flame as measured with an FTIR spectrometer.

Although the objective of these experiments was to measure hydrocarbons, it should be pointed out that the simpler molecules, such as CO, CO_2, H_2O, and perhaps even OH, were easily observed, even in the highly sooting parts of the flame. The dominant source of noise in these experiments seemed to be flame fluctuations, not soot particles. It is not anticipated that larger particles, such as pulverized coal, would present a serious measurement problem.

These experiments are being continued with the surface mixing burner previously used in the Raman experiments; with propane as a fuel, it can be operated either as a sooting premixed or diffusion flame.

Laser Absorption and Mass Spectroscopy of the OH Radical - R. Cattolica

A comparison of laser absorption and mass spectroscopy measurements on the concentration of the OH radical in atmospheric pressure flames has been conducted in cooperation with Professor Eldon Knuth of the Department of Chemical, Thermal, and Nuclear Engineering at the University of California in Los Angeles. Using molecular beam mass-spectroscopy, Professor Knuth's research group has made a systematic study of the effect of nozzle design characteristics on both stable and radical species concentrations in an atmospheric methane-air flat flame. Complementary absorption measurements of the OH radical concentration profiles, using a tunable dye laser, have

been completed at SNLL in the same type of flame under identical conditions. Temperature profiles through the flame were determined with a time-of-flight technique using the mass spectrometer at UCLA. Thermocouple measurements of the temperature profiles were taken at both UCLA and SNLL to insure that identical flames were used in the comparison.

Preliminary results indicate that the time-of-flight temperature measurement yields accurate results only in the post-flame gas region. Substantial perturbation of the temperature and OH concentration profiles through the flame transition zones indicated nozzle interference effects. A joint research report on this study is in preparation and will be presented at the 1980 Fall meeting of the Western States Section of the Combustion Institute, University of Southern California, October 20-21, 1980.

The Role of the OH Radical in Catalytic Combustion - R. Cattolica

In cooperation with the combustion research group (under Dr. Frank Robben) at the Lawrence Berkeley Laboratory, a joint experiment is being conducted on the role of the OH radical in catalytic combustion. Dr. Robert Schefer of LBL has brought a catalytic flat plate experiment to SNLL to use the laser fluorescence capabilities for making OH concentration measurements of the OH radical in the laminar boundary layer of a lean hydrogen-air mixture flowing over a platinum surface heated to 1300°K. Modeling of the combustion processes in this environment requires a knowledge of the effect of the boundary conditions on the fate of the OH radical. With the results of the current investigations, Dr. Schefer will be able to evaluate the use of various boundary conditions in his numerical model of the experiment.

Ammonia/Oxygen Flame Studies - R. M. Green/J. A. Miller

Concentration profiles of the NH_2 radical have been measured in rich, stoichiometric, and lean premixed NH_3/O_2 flames at low pressures using laser absorption spectroscopy. It has been postulated that a large shear-induced mixing layer at the boundary of the flame was creating an inhomogeneity in the laser optical path resulting in an unrealistically rapid decay of the measured translational temperature of the post-flame gases. These effects have been minimized through the use of a momentum-flux matched co-flow of nitrogen at the flame boundary. Comparisons of the translational temperatures with radiation-corrected themocouple measurements (made well away from the boundary of the flame) have verified the adequacy of the solution.

The translational temperature distribution exhibited a problem in the initial data reduction. As one moved further downstream from the burner in the post-flame region, the translational temperatures exhibited an increasing amount of scatter which quickly became unacceptable. Since the inferred NH_2 concentration was obtained from the integrated absorption coefficient and the temperature profile, the scatter in the temperature was transferred to the concentration profile. A careful consideration of the experimental absorption spectra illustrates the cause of the scatter in the temperature data. In the post-flame region, where the NH_2 concentration rapidly decreases to a low level, the absorption lines were quite weak in addition to being

broadened by a high temperature. As a result, the absorption line profiles were poorly resolved thus reducing the precision of the data fitting technique which used these profiles to obtain a translational temperature. This problem was overcome by using the translational temperatures only in the region close to the burner in the reaction zone where NH_2 concentrations were highest and precise fitting of the profiles was possible. In the post-flame region the thermocouple measurements were used to smooth the scattered translational temperatures. The use of these "smoothed" temperature profiles in the calculation of the NH_2 concentration resulted in concentration profiles which exhibit nearly no data scatter, illustrating the sensitivity of the measured integrated absorption coefficient at a low concentration of absorbing species.

Figures 5, 6, and 7 illustrate relative concentration and temperature profiles for rich, stoichiometric, and lean NH_3/O_2 flames. Note that the relative concentration plotted in the figure is the product of the absolute mole fraction of NH_2 and the oscillator strength, f, of the transition used in obtaining the absorption spectra. Although f is not known, the relative profiles still contain valuable information. The shape of the profiles and the position of the peaks are being used to verify the adequacy of reaction mechanisms through comparisons with flat-flame code predictions which are made using finite-rate chemistry.

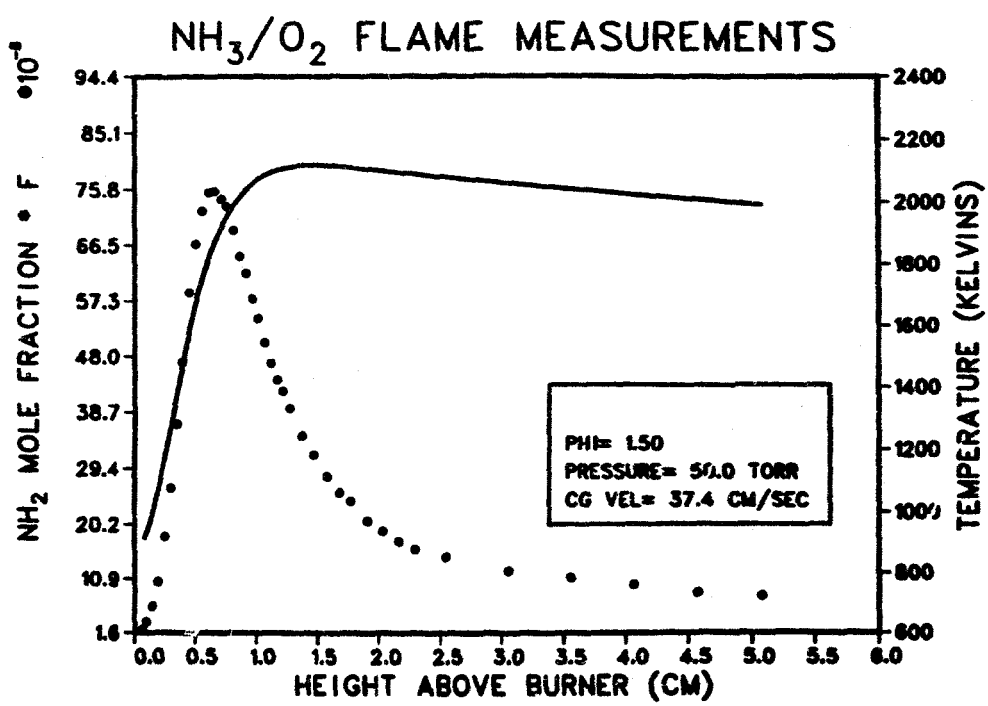

Figure 5: Relative Mole Fraction and Temperature Profiles in a Rich NH_3/O_2 Flame.

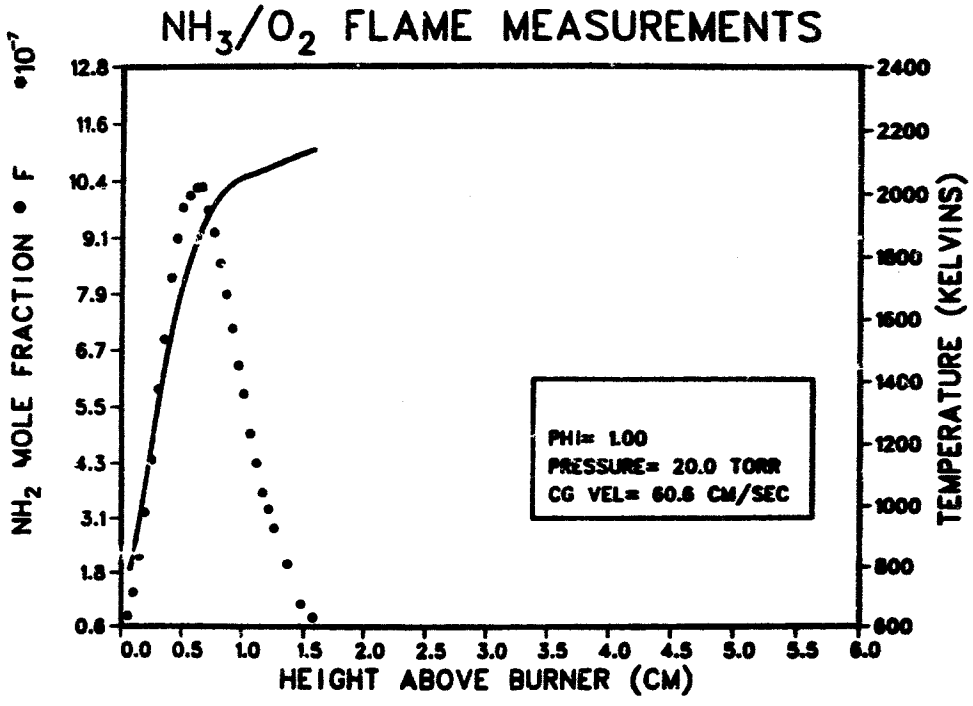

Figure 6: Relative Mole Fraction and Temperature Profiles in a Stoichiometric NH_3/O_2 Flame.

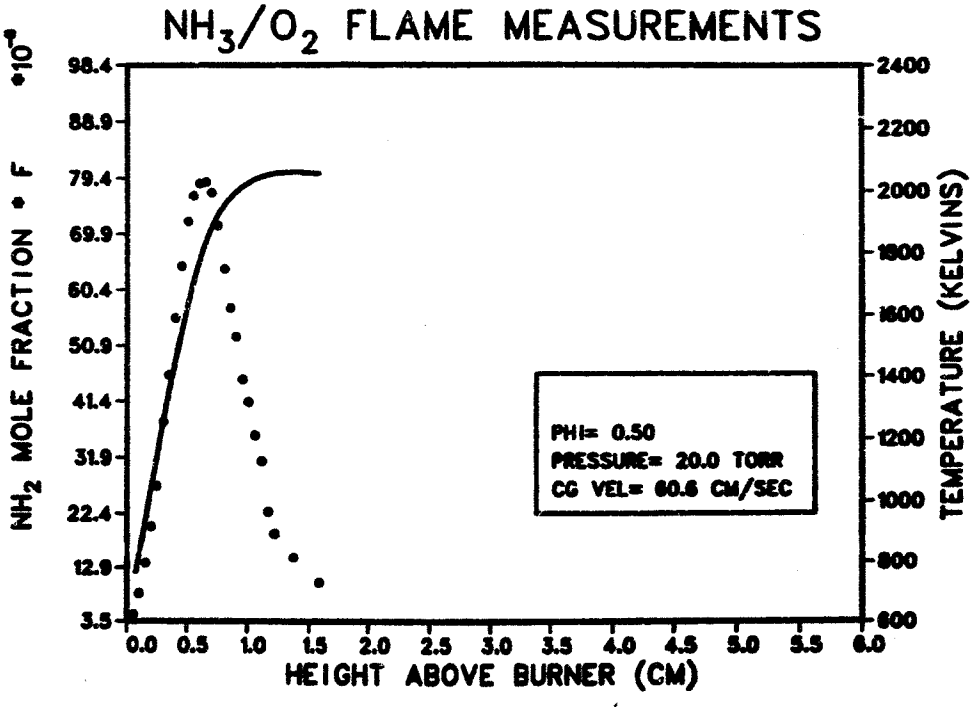

Figure 7: Relative Mole Fraction and Temperature Profiles in a Lean NH_3/O_2 Flame.

Model for Diffusion-Controlled Reduction of Nitric Oxide by Ammonia - J. A. Miller/R. J. Kee/M. C. Branch (Univ. of Colorado)

In order to understand the selective reduction of nitric oxide by ammonia under non-homogeneous conditions, calculations have begun to model the experiments conducted by Banna at the University of Colorado. In these experiments, two co-flowing streams were mixed. The outer stream consists of post-flame combustion products containing superequilibrium NO diluted in argon. The inner stream contains ammonia diluted in argon. As they mix, reaction occurs between the NH_3 and NO. In order to solve this problem, the diffusion flame model of Kee and Miller (transformed to stream function coordinates, the transport and chemical kinetics terms coupled, and provision made for including an outer wall by including a pressure gradient term) has been modified and a version of the reaction mechanism of Miller, Branch, and Kee adopted.

Figure 8 shows the result of a preliminary calculation for NH_3 decay along the centerline of the co-flowing streams. The agreement is acceptable for a preliminary calculation. Better agreement can probably be obtained by a more precise specification of conditions at the burner exit plane and by including a more complete reaction mechanism. An interesting point that comes out of these calculations is that the optimum temperature for NO reduction moves to a higher temperature than under homogeneous plug-flow conditions. The ability of chain carriers to diffuse away from the active reaction zone severly limits the chain branching mechanisms.

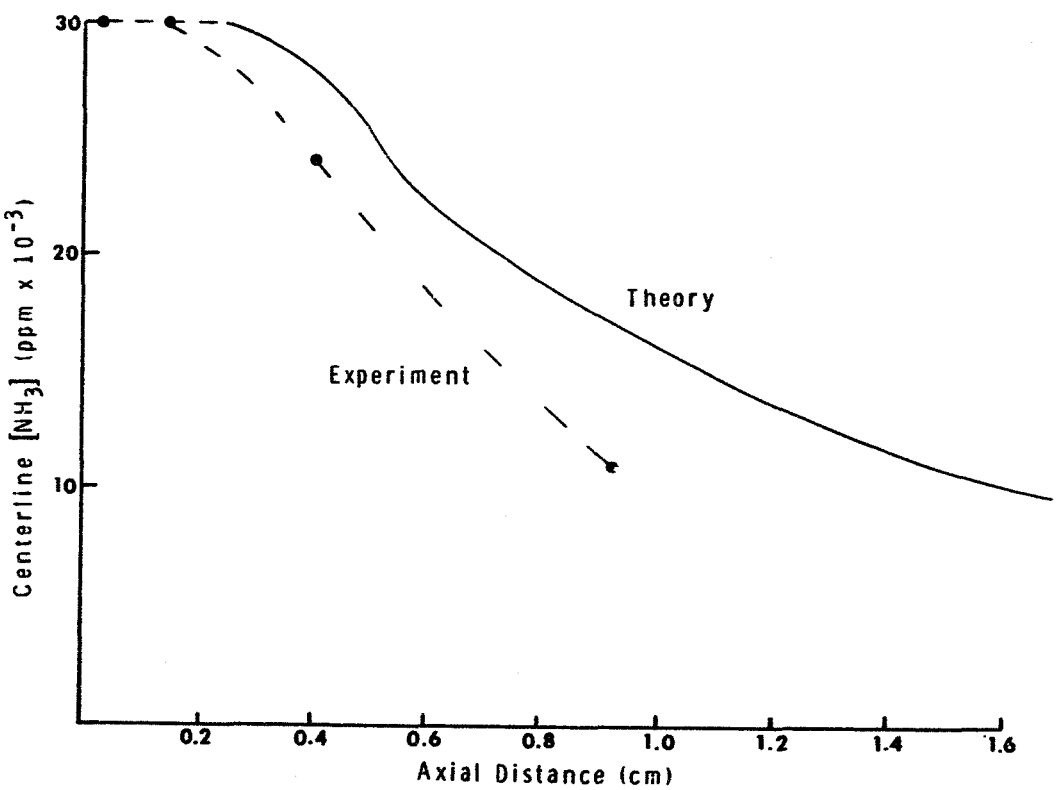

Figure 8: A calculation of $[NH_3]$ along the centerline of a co-flowing stream of NO and NH_3.

Confined Axisymmetric Turbulent Jet - R. E. Mitchell

The k-ε model of turbulence was checked for its internal consistency and it was found that two of the "empirical constants," C_{ε_1} and C_{ε_2}, must satisfy prescribed relations. The k-ε model is given by

$$\nabla\cdot\left[\rho\bar{u}k - \frac{\mu^{(t)}}{\sigma_k}\nabla k\right] = \mu^{(t)}\,G - \rho\varepsilon \tag{1}$$

$$\nabla\cdot\left[\rho\bar{u}\varepsilon - \frac{\mu^{(t)}}{\sigma_\varepsilon}\nabla\varepsilon\right] = C_{\varepsilon_1}\,\mu^{(t)}\left(\varepsilon/k\right)G - C_{\varepsilon_2}\,\rho\varepsilon^2/k \tag{2}$$

where the turbulent viscosity is defined as

$$\mu^{(t)} = C_\mu\,\rho k^2/\varepsilon \tag{3}$$

The five constants in the model (C_μ, σ_k, σ_ε, $C_{\varepsilon 1}$, and $C_{\varepsilon 2}$) were determined by comparisons of experiment and calculation. Values recommended by Launder are,

$$C_\mu = 0.09 \quad \sigma_k = 1.0 \quad \sigma_\varepsilon = 1.3 \quad C_{\varepsilon_1} = 1.45 \quad C_{\varepsilon_2} = 1.92$$

Satisfactory predictions has been reported for a variety of boundary layer type flows when these values are used. The values cannot be considered to be universal constants for it is necessary to modify two of these (C_μ and C_{ε_2}) when considering the round jet.

Equation (3) can be rearranged to give

$$\varepsilon = C_\mu\,\rho k^2/\mu^{(t)}. \tag{4}$$

Using this equation, $\nabla\cdot(\rho\bar{u}\varepsilon)$ and $\nabla\cdot\left(\frac{\mu^{(t)}}{\sigma_\varepsilon}\nabla\varepsilon\right)$ can be determined as functions of $\nabla\cdot(\rho\bar{u}k)$, $\nabla\mu^{(t)}$, $\nabla\cdot\nabla\mu^{(t)}$, and $\nabla\cdot\nabla k$. The terms $\nabla\cdot(\rho\bar{u}k)$ and $\nabla\cdot\nabla k$ can be eliminated by employing Eq. (1). By forming the expression $\nabla\cdot\left[\rho\bar{u}\varepsilon - \frac{\mu^{(t)}}{\sigma_\varepsilon}\nabla\varepsilon\right]$, using the functions derived, comparison with Eq. (2) indicates that

$$C_{\varepsilon_2} = 2.0 \tag{5}$$

and

$$C_{\varepsilon_1} = 2 + \frac{1}{\mu^{(t)}G}\left\{2\left(1 - \frac{\sigma_k}{\sigma_\varepsilon}\right)\nabla\cdot\left(\frac{\mu^{(t)}}{\sigma_k}\nabla k\right) + \frac{2\mu^{(t)}}{\sigma_\varepsilon}\left(\frac{2}{\mu^{(t)}}\nabla\mu^{(t)} - \frac{1}{k}\nabla k\right)\cdot\nabla k\right.$$
$$\left. + \frac{k}{\sigma_\varepsilon}\nabla\cdot\nabla\mu^{(t)} - \frac{k}{\mu^{(t)}}\left(\rho\bar{u} + \frac{1}{\sigma_\varepsilon}\nabla\mu^{(t)}\right)\cdot\nabla\mu^{(t)}\right\} \tag{6}$$

Using this expression for $C_{\varepsilon 1}$ adds no more complexity to the k-ε model of turbulence, since Eqs. (1), (2), and (3) must be solved simultaneously irrespective of the value of $C_{\varepsilon 1}$ used.

The k-ε model of turbulence can thus be considered to consist of only three empirical constants: C_μ, σ_k, and σ_ε. $C_{\varepsilon 2}$ and $C_{\varepsilon 1}$ are given by Eqs. (5) and (6) above. Tests are presently underway to determine values of C_μ, σ_k, and σ_ε which can be used for all flow situations.

Turbulent Diffusion Flame Facility (TDFF) - G. D. Rambach

The Turbulent Diffusion Flame Facility is currently configured to accommodate mixtures of hydrogen and gas phase methanol. The mixtures are required to satisfy the requirements of a Rayleigh scattering temperature measurement for diffusion flames. For the proper fraction of methanol in hydrogen, the Rayleigh scattering cross section is essentially the same for the reactants and products, yielding a simple measurement of temperature. Since the appropriate methanol fraction in the fuel corresponds to a saturation temperature of 40°C, the hydrogen was bubbled through a volume of liquid methanol heated to the correct temperature. All the downstream fuel plumbing was heated to at least 50°C to avoid condensation of the methanol before injection into the test section.

The cyclone seeder previously used to inject particles into the hydrogen fuel jet was heated to about 60°C to permit seeding of the methanol/hydrogen mixture with Al_2O_3 particles without them acting as condensation sites. However, since the fuel mixture was used to scavenge the particles from a packed bed, the large hydroscopic surface area of particles exposed to the fuel appeared to preferentially absorb enough methanol to alter its concentration and the Reynolds number of the fuel jet. After a short period of operation, dispersion of the particles in the seeder was not possible. This problem of seeding the fuel jet will soon be circumvented with the use of an evaporator that injects methanol into a hot, preseeded hydrogen stream.

The two color LDV receiving optics have been retrofit with improved lenses which increased the signal-to-noise in the present configuration from two to about ten. Two-component velocity measurements in a CH_3OH/H_2 turbulent diffusion flame have been initiated along the same radial traverses as previous Rayleigh temperature measurements. The LDV seed is only being injected into the air side, but the measurements are being taken far enough downstream that a complete radial traverse can be made. Turbulent flames with jet Reynolds numbers of 5000 and 8000 are being investigated.

The FORTRAN program for data collection and reduction on the PDP 11/34 has been extended to transfer the raw data for 3000 measurements of U_i, V_i, and t_i to a disc file for each spatial location. The raw data is stored in a fashion that is compatible with the CDC 6600 to minimize transfer time to magnetic tape.

A Schlieren system has been fabricated for the TDFF that will be used for high speed movies of turbulent flames. The Schlieren system should give better resolution of the flame structure and represent the location of the

flame boundary more accurately than the shadowgraph system used in earlier experiments. The Schlieren movies will be compared with velocity and temperature measurements to improve the understanding of the processes that occur in these flames and to help define the types and methods of experiments to be used in the future.

Turbulent Reacting Flow Studies - R. W. Bilger/R. W. Dibble

Professor R. W. Bilger of the Department of Mechanical Engineering, University of Sydney, Australia, has been visiting for three months. Turbulent diffusion flame problems have been the central topic of discussion. Plans for the new turbulence/chemistry interaction studies laboratory in the facility have received considerable attention. The Sydney University computer code for turbulent diffusion flames has been modified for use on the Sandia computer and has been used to predict certain of the flames measured at Sandia. A theory for differential diffusion due to molecular transport has been developed and an experiment designed to test the theory by using Rayleigh scattering from a jet of propane and hydrogen mixing in air; a preliminary experiment has yielded encouraging results. The theory has also been used to predict molecular transport effects in the mildly turbulent diffusion flame of Lapp and Drake at GE in Schenectady with good agreement. The large effects on temperature and composition found in these experiments can now be avoided in the design of experiments to elucidate turbulent/kinetics interactions. Professor Bilger also gave a series of seminars on turbulent-non-premixed combustion.

MOLECULAR PHYSICS AND SPECTROSCOPY

The studies in this section are concerned with detailed molecular physics relevant to chemically reacting systems and the calculation of transport coefficients of chemical species in a multicomponent gaseous environment. Detailed spectroscopic studies will be reported in this section.

Observation of an Optical Stark Effect on Vibrational and Rotational Transitions - L. A. Rahn/R. L. Farrow/M. L. Koszykowski/P. L. Mattern

The first observation of shifts in molecular rotational and vibrational frequencies induced by an optical field has been observed; the field was not resonant with molecular transition frequencies. The Stark shifts of rotational transitions in polar molecules have been studied extensively using low frequency applied fields.(1) Stark shifts of vibrational frequencies driven near resonance have been investigated,(2) but shifts due to the presence of nonresonant optical fields have not been reported previously.

In the experiments described here, a frequency shift of the S(3) rotational transition in molecular hydrogen was observed in coherent anti-Stokes Raman scattering (CARS). The spectra was obtained from a sample volume irradiated

by the focused output of a pulsed 1.06 μm Nd:YAG laser. A shift of 0.12 cm^{-1} to lower frequency is measured for the data shown in Fig. 9 for the perturbed spectrum (crosses) compared to the unperturbed spectrum (circles). The data were obtained using a high-resolution (0.1 - 0.2 cm^{-1}), time-averaged, crossed-beam CARS apparatus. Spatial resolution was obtained by crossing two focused 532.0 nm pump beams in the horizontal plane such that they intersected a probe laser beam contained in the vertical plane. For each data point, 50 single-shot measurements were digitized, normalized, and averaged. The perturbing optical field was provided by the 1.06 μm output ("infrared" beam) of the 'Q'-switched Nd:YAG laser. By blocking alternate infrared laser pulses with a 5 Hz chopper, perturbed and unperturbed spectra were averaged simultaneously. This process essentially eliminated wavelength uncertainties between the two spectra. As a result of the spatial and temporal resolution of the CARS experiment, relatively small variations in the high power infrared field intensity occurred during the generation of the CARS signal. For the measurements of Fig. 9, the infrared laser pulse energy was typically ∿200 mJ, measured after the focusing lens, and the probe and pump laser pulse energies were 0.4 mJ and 3 mJ, respectively. CARS experiments have also been performed in which the Stark shift is caused by a high power pump laser. Asymmetrically broadened line-shapes in both vibrational and rotational spectra were observed, presumably due to gradients in the optical field of the pump laser.

The observed frequency shifts are interpreted by considering the coupling of the optical field to the molecule <u>via</u> the variation of the electronic polarizability with internuclear separation. The primary effect of the perturbation is to increase the equilibrium internuclear spacing, q_e. The theoretical change in rotational frequency can be calculated from the change in the moment of inertia, and is given to first order by

$$\delta\omega_r = -\omega_r^o \frac{E_o^2}{4D_e\beta^2 q_e} \left(\frac{d\alpha}{dq}\right)_{q_e} ,$$

where ω_r^o is the unperturbed frequency, E_o is the field amplitude, α is the polarizability (assumed to be isotropic), and $2D_e\beta^2$ is the harmonic force constant for a Morse oscillator. The vibrational frequency shift is calculated from the change in the harmonic force constant, and is given to first order for the ground state by

$$\delta\omega_v = -\omega_v^o \frac{3E_o^2}{16D_e\beta} \left(\frac{d\alpha}{dq}\right)_{q_e} ,$$

where ω_v^o is the unperturbed vibrational frequency. These expressions have been compared with exact numerical solutions of the time independent Schroedinger equation; less than a five percent error was found for H_2 with fields up to 10^{13} W/cm^2.

An estimate of the peak intensity due to the 200 mJ, 1.06 μm Q-switched pulse used in the experiment indicates 8(±4) x 10^{11} W/cm^2. Using this value and a polarizability derivative for H_2 of 1.2 $Å^2$, the predicted

rotational shift is -0.11(±.05) cm^{-1}. Thus, the observed -0.12 cm^{-1} line-shift is consistent with the calculation. The observed shift is an order of magnitude larger than the estimated collisional width of hydrogen at one atmosphere. A consideration of this Stark shift is important for high resolution laser spectroscopy, even at much lower power densities. It is anticipated that this perturbation will also be important in some infrared laser photolysis experiments and their application to isotope separation. Finally, experiments are in progress to demonstrate spatially-resolved infrared absorption utilizing this form of Stark effect to modulate the absorption frequency of ammonia.

REFERENCES

1. C. H. Townes and A. L. Schawlow, Microwave Spectroscopy (McGraw-Hill, New York, 1955).

2. C. D. Cantrell, S. M. Freund, and J. L. Lyman, in Laser Handbook, M. Stitch, ed. (North-Holland, Amsterdam, 1978), Vol. 3.

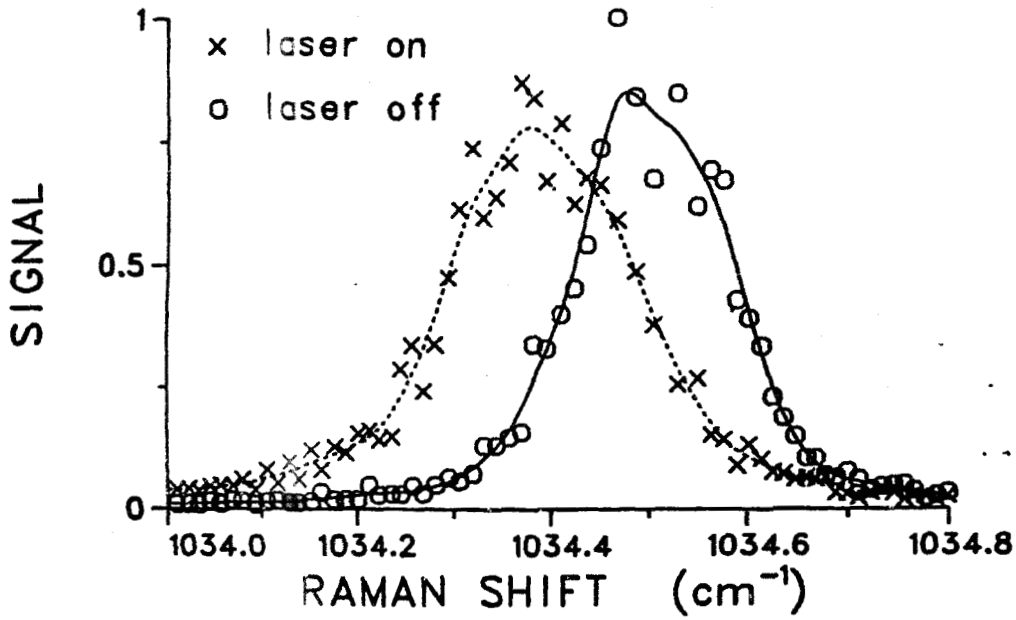

Figure 9: The effects of high intensity infrared radiation on the position and lineshapes of the S(3) rotational transition of molecular hydrogen. The solid and dashed lines are smooth curves drawn through the data points.

Kinetics of Soot Precursers by XUV Spectroscopy - R. W. Schmieder

The spectrum of visible fluorescence from acetylene gas (C_2H_2) irradiated with XUV photons has been recorded for the first time. Figure 10 shows a typical spectrum obtained in a single scan of 2 hours' duration. The XUV source was a microwave discharge in Ne at 300 mTorr, which provided the NeI λ73.6 nm line. The fluorescence from C_2H_2 at 600 mTorr was dispersed with a 1/4-m monochromator and detected with a cooled EMI 6256 photomultiplier. The spectral resolution was about 1 nm.

The spectra show the Swan bands of C_2 including the $\Delta v = -1, 0, +1$ sequence and two bands of CH, the blue-violet ($A\ ^2\Delta$ - $X\ ^2\Pi$) with the head at 4315 nm, and the near ultraviolet ($B^2\Sigma^-$ - $X\ ^2\Pi$) band.

The energy of the Ne line (16.8 eV) is just below the appearance potential for the ethynyl ion (C_2H^+) which may be a precursor of C_2 and CH. Future efforts will be made to observe a possible change in these spectra associated with this threshold.

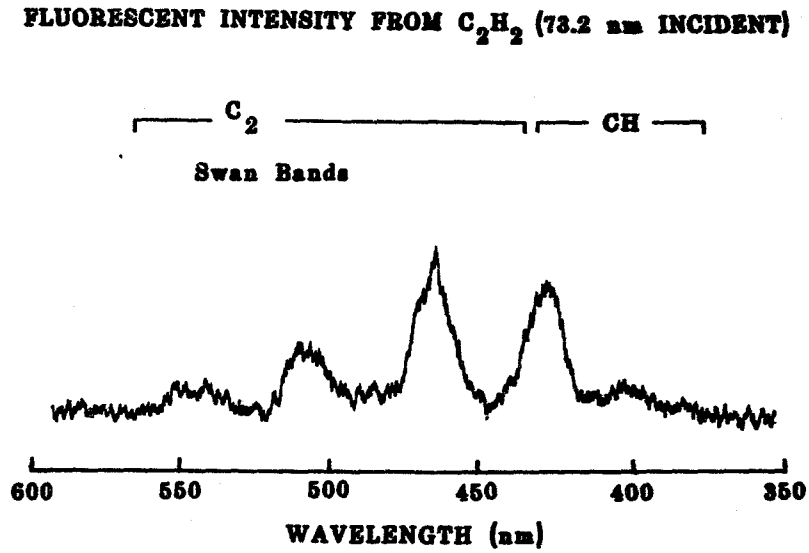

Figure 10: Fluorescence spectrum in the visible from acetylene irradiated by VUV radiation (73.6 nm).

High Temperature Raman Measurements of CO_2 and H_2O - D. A. Stephenson

The high temperature measurements of the Raman spectra of CO_2 and H_2O have been completed. The observed spectra confirmed the theoretical models used to predict these spectra. In particular, it was found that the simple harmonic oscillator-rigid rotor partition functions can be used, even at temperatures as high as 2100 K.

The spectra were measured in the hot post-flame gases of the surface mixing burner described previously. The oxidant was a 2:1 mixture of N_2 and O_2 to insure lean operation even at high flame temperatures. The temperature was

adjusted primarily by varying the input methane flow; however, to obtain the lowest temperatures it was necessary to extract heat with metal screens above the flame, but below the measurement region. The rapidly pulsed Nd:YAG laser and gated CAMAC electronics minimized the observed background luminosity from the flame.

Figure 11 shows the amount of product (CO_2 or H_2O) measured in the flame divided by the amount of fuel as functions of temperature. The ratios of both the products and the fuel relative to nitrogen were used in order to avoid calibration problems. Similarly the absolute values of the products have been normalized; it is only the temperature dependence that is of interest here. The results show no discernible trend with temperature, nor is there any significant difference between the data taken with the nitrogen shield (squares) from those taken with argon shield (circles).

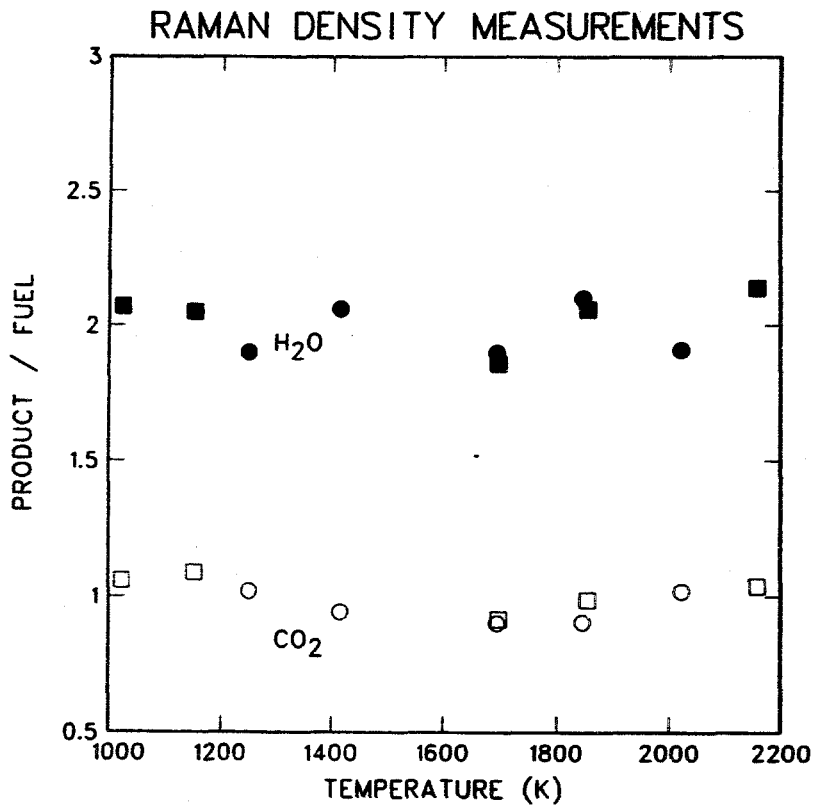

Figure 11: The normalized concentrations of CO_2 and H_2O measured in the postflame gases of a $N_2/O_2/CH_4$ flame. The mixture was lean in all cases so that the CH_4 should go over quantitatively to CO_2 and H_2O independent of temperature, as the measurements confirm.

On Correlation Functions and Normal Modes - M. L. Koszykowski

In unimolecular reactions, chemical activation experiments, infrared multiphoton dissociation, and vibrational spectroscopy, a bond (or group of bonds) is vibrationally excited by collision, chemical reaction, or optical radiation. The rate at which this energy is transferred to other bonds and to other molecules is of interest in regard to the interpretation of chemical reactions. It is often assumed in reaction rate theory that the intramolecular relaxation occurs on a time scale short compared with the mean time for subsequent reaction of the molecule. It has been demonstrated that moments of correlation functions[1] accurately describe intermolecular relaxation and spectroscopic linewidths. This report documents preliminary results of an investigation of intramolecular relaxation.

The Hamiltonian used is

$$H = \frac{1}{2m_x} P_x^{\,2} + \frac{1}{2}\omega_x^2 x^2 + \frac{1}{2m_y} P_y^{\,2} + \frac{1}{2}\omega_y^{\,2} y^2 + \lambda(xy^2 - \eta y^3),$$

which represents two normal modes with nonlinear coupling. The correlation function is defined as

$$C(t) = \langle E_x(0)E_x(t)\rangle ,$$

where $E_x(t)$ is the energy in the x mode at t (t = 0 is the time of excitation). If the normal coordinates are a "good" representation, the correlation function should be constant, and statistical reaction theories will not be valid. On the other hand, if there is total relaxation, one should find

$$C(\infty) = \langle C(0)C(\infty)\rangle = \langle C\rangle^2 = 3/4 \text{ and } C(0) = \langle C^2\rangle = 1 .$$

In this case, C(t) will decay from 1.0 to 3/4. This result is precisely what is found using a correlation function approach in Fig. 12. In this analysis the relaxation time is related to an energy diffusion time and may be useful in bridging the gap between Slater's unimolecular reaction theory (normal modes) and RRKM theory (totally random energy distributions). This relaxation will also give rise to interesting lineshapes of reaction intermediates. The application of these correlation function techniques to H_2O and the local model-normal mode question is being pursued.

REFERENCE

1. M. E. Coltrin, M. L. Koszykowski, and R. A. Marcus, J. Chem Phys., in press.

   L. A. Rahn, A. Owycung, M. E. Coltrin, and M. L. Koszykowski, International Raman Conference, 1980.

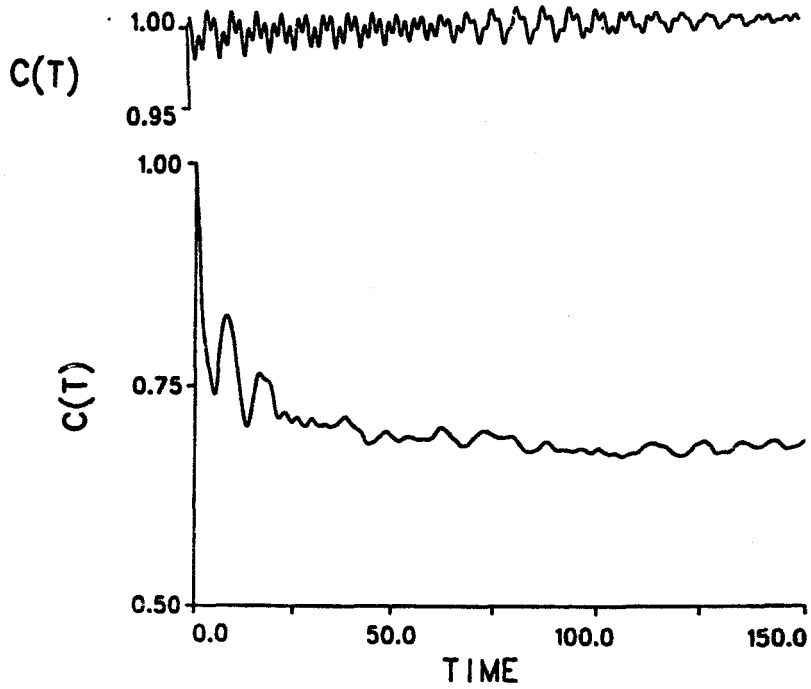

Figure 12: Normal coordinate correlation function a) for a "good" coordinate b) a mode showing vibrational relaxation.

DIAGNOSTICS RESEARCH

The studies reported in this section relate to new approaches, primarily optical, for the diagnostics of combustion as well as a continuing evaluation and improvement of existing techniques.

Two-Line Laser Excited Fluorescence Temperature Measurement - R. Cattolica

A temperature measurement technique using two-line laser excited fluorescence (LEF) has been developed. The rotational temperature of the OH molecule has been measured using this method. The approach consists of exciting two different rotational vibronic transitions from the ground state to a common excited rotational vibronic state. The resulting fluorescence is monitored and the ratio, R, of the resulting emissions formed. Figure 13 illustrates the laser fluorescence profiles across a methane-air (ϕ = 1.0) flat-flame. The asymmetry of the fluorescence profiles indicates the effect of radiation trapping. The fluorescence ratio, however, is independent of the fluorescence trapping. This ratio, R, is also independent of quenching and any non-equilibrium population distribution in the excited state. This latter effect also makes it independent of the spectral bandwidth of the detection system. The rotational temperature, T_r, can be easily calculated from the relationship

$$T_r = \frac{-\frac{hc}{k}\Delta E}{\ln\left(R\,\frac{g_1}{g_{1'}}\,\frac{B_{21}}{B_{21'}}\right)}\,, \qquad (1)$$

where ΔE is the energy level difference between rotational states (1) and (1′) in the $X^2\Pi(v'' = 0)$ ground state of the OH molecule. The degeneracies g_1 and $g_{1'}$ of the two ground states and the Einstein coefficient for absorption to the rotational state (2) in the $A^2\Sigma(v' = 0)$ state are known for the OH molecule. The temperature fluctuations in Fig. 13 are consistent with the Poisson statistical character of the fluorescence intensity measurements. The sensitivity of the inferred temperature to the ratio of the fluorescence intensities can be determined by using higher rotational levels or by pumping from two different vibrational levels in the ground electronic state. A detailed discussion of this technique including conclusions with regard to the possibility of temperature measurements in turbulent combustion environments can be found in a Sandia report (SAND79-8831).

OH TWO-LINE LASER FLUORESCENCE TEMPERATURE
IN A METHANE-AIR FLAT FLAME

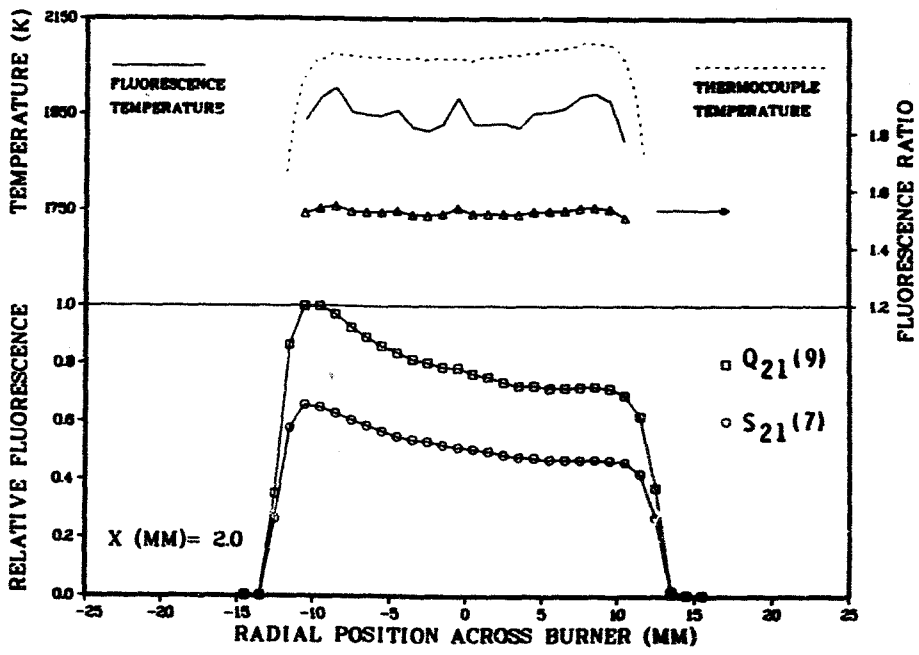

Figure 13: Two-line laser excited fluorescence (LEF) temperature profile of the OH molecule 2 mm above a methane-air flat flame burner. The $Q_{21}(9)$ and $S_{21}(7)$ transitions were excited with a tunable dye laser operating in the ultraviolet (∿300 nm). Also shown is a thermocouple profile taken at the same position.

Scattered Light - Free Combustion Kinetics - F. P. Tully

Chemical reaction rate data at temperatures relevant to combustion have been obtained almost exclusively through indirect methods, such as the kinetic modeling of experimental measurements on complex reactive systems. Sequences of reaction schemes with parameterized rate coefficients are used to iteratively reproduce the measured concentration profiles and/or product yields.

In contrast, direct studies which monitor reactant disappearance or product formation in isolated elementary reactions have been scarce at temperatures above 500K. The most promising technique of making unambiguous direct kinetic measurements of elementary reactions at temperatures as high as 1800K is the laser photolysis - laser induced fluorescence method. Briefly, a homogeneous gas-phase reaction is initiated by a short duration laser photolysis pulse. The rate of decay or growth of the resultant transient species are followed via time-resolved electronic absorption or fluorescence. However, absorption measurements are frequently plagued by the detectivity requirement of large radical concentrations, which encourage secondary reactions. Fluorescence experiments are typically limited by the ability to discriminate between fluorescence of transient species and the scattered light signal from the cw exciting beam.

The first allowed electronic transitions for a large number of important combustion intermediates are located in the ultra-violet at wavelengths inaccessible to conventional cw dye lasers. Excitation laser probes for efficient kinetic studies of the reactions of species such as OH, NH, CH_3, CN, SH, SO, S_2, etc., do not exist. This report summarizes the results of a feasibility study to develop uv sources appropriate for combustion-related fluorescence experiments.

The use of a mode-locked, cavity-dumped, synchronously-pumped picosecond dye laser system as an excitation source has been investigated. Calculations and measurements demonstrate a variety of interesting features:

1) The second harmonic power generation varies as the square of the laser power at the fundamental wavelength. Pico-second pulses generate far greater peak power densities than those obtainable cw. Calculations predict that second harmonic conversion efficiencies in excess of 10% are feasible. The photon flux thus obtainable exceeds that from a conventional resonance lamp by a factor of 3-10.

2) The laser pulse repetition rate in the cavity-dumped configuration is typically $\sim$1 MHz. Given the time scale on which the chemistry is proceeding ($\sim$ 1 msec), this rapid pulsing is equivalent to a cw probe for the experiment. Thus, contributions to a complete decay curve may be signal averaged for each photolysis pulse; initiating pulse power variations can be ignored.

3) Under the conditions of a typical experiment, the fluorescent lifetimes of the emitting transient species range from 50-500 nsec. Running the cavity-dumper at a 1 MHz repetition rate and triggering off each probe pulse, it is possible to use gating techniques to discriminate against scattered light coming from the picosecond

excitation probe pulse. Experimental measurements have shown that the product of the laser pulse duration and the spectral linewidth of the visible laser output is approximately Fourier transform limited, i.e., a 10 ps pulse possesses a frequency spread of ∿ 45 GHz. Computer calculations performed at SNL and plotted in Fig. 14 demonstrate that the typical laser output linewidth is smaller than the efficiently phase-matched frequency bandwidths of two prominent non-linear crystals throughout their entire temperature tuning range. Relatively high second harmonic generation efficiencies are thus assured. Currently, a pico-second laser system optimized for the detection and characterization of OH is being designed.

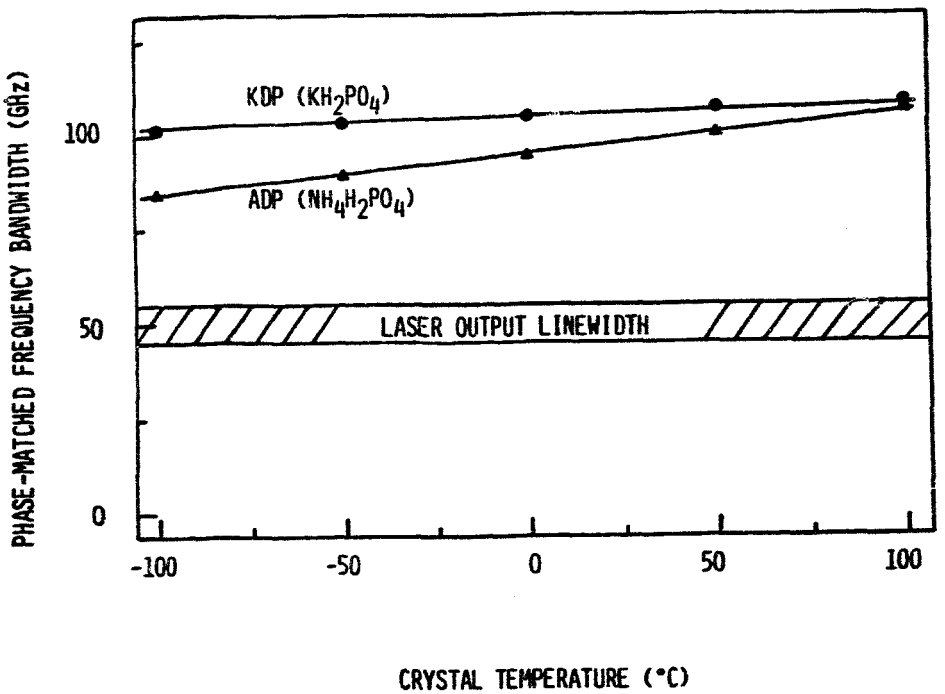

Figure 14: The frequency bandwidth of KDP and ADP crystals as a function of crystal temperature.

PRESENTATIONS

1. R. M. Green, "Work in Progress," report at Spring Meeting of the Western States Section of the Combustion Institute at Newport Beach, CA, April 1980.

2. R. M. Green, Status Report on Diesel Combustion Research at SNLL, "Measurement of NH_2-Radical in NH_3/O_2 Flames," at Cummins Engine Co., Columbus, IN, May 1980.

3. R. M. Green, "Measurement of NH_2 Radical Relative Concentration Profiles in an NH_3/O_2 Flame Using Laser Absorption Spectroscopy," Thirty-Fifth Symposium on Molecular Spectroscopy, Ohio State University, OH, June 17-20, 1980.

4. G. D. Rambach, "Laser Doppler Velocity Measurements in Turbulent Flames," presented at the Workshop on Turbulent Combustion, Desert Research Institute, Las Vegas, NV, April 23-25, 1980.

5. R. W. Dibble/R. E. Hollenbach, "CW and Pulsed Laser Rayleigh Thermometry Applied to Turbulent Combustion," presented at 35th Symposium on Molecular Spectroscopy, Columbus, OH, June 16-20, 1980. (N.B. paper delivered by R. J. Cattolica.)

6. R. W. Dibble/R. E. Hollenbach/G. D. Rambach, "LDV and Rayleigh Thermometry in Turbulent Flames," presented at University of Nevada, Desert Research Institute Workshop on Turbulent Combustion, April 23, 1980.

7. D. L. Hartley, "Spectroscopic Needs for Combustion Diagnostics," presented at the 35th Symposium on Molecular Spectroscopy, Ohio State University, Columbus, OH, June 16-20, 1980.

8. R. J. Cattolica, "OH Rotational Temperature from Two-Line Laser Excited Fluorescence," 35th Annual Symposium on Molecular Spectroscopy, June 16-20, 1980, Ohio State University, Columbus, OH.

9. D. L. Hartley/M. A. Gusinow, "Applications of Optical Diagnostic Techniques in Combustion Research," presented at the Advisory Group for Aerospace Research & Development meeting in Brussels, Belgium, May 5-7, 1980.

10. D. L. Hartley, "Combustion Research at Sandia," Seminar, Georgia Tech, May 9, 1980.

11. R. L. Farrow/M. L. Koszykowski/P. L. Mattern/L. A. Rahn, "Effects of High Optical Powers on CARS Spectra," 35th Annual Symposium on Molecular Spectroscopy, June 16-20, 1980, Ohio State University, Columbus, OH.

PUBLICATIONS

1. R. E. Mitchell, "A Theoretical Model of Chemically Reacting Recirculating Flows," SAND79-8236, April 1980.

2. R. W. Dibble, R. E. Hollenbach, and G. D. Rambach, Laser Probes for Combustion Chemistry, D. R. Crosley (ed.) Chapter 56 American Chemical Society Symposium Series, to be published Spring 1980.

3. R. J. Cattolica, D. Coe, F. Robben and L. Talbot, "Rotational Temperatures in Nonequilibrium Free Jet Expansions of Nitrogen," Physics of Fluids, vol. 23, no. 4, pp. 706-714, April 1980.

4. R. J. Cattolica, D. Coe, F. Robben and L. Talbot, "Measurements of Translational Temperature in Nitrogen with the Electron Beam Fluorescence Technique," Physics of Fluids, vol. 23, no. 4, pp. 715-718, April 1980.

5. R. J. Cattolica, "OH Rotational Temperature from Two-Line Laser Excited Fluorescence," Sandia Technical Report, SAND79-8831, June 1980.

INITIAL DISTRIBUTION

W. G. Agnew
Technical Director
General Motors Research Laboratories
Warren, MI 48090

W. Bartok
Senior Research Association
Exxon Research and Engineering Corporation
P. O. Box 8
Linden, NJ 07036

H. B. Palmer
College of Earth and Mineral Sciences
Fuel Science Section
Department of Materials Science
and Engineering
The Pennsylvania State University
101 Mineral Industries Building
University Park, PA 16802

S. S. Penner
Department of Engineering Physics
University of California at San Diego
P. O. Box 109
La Jolla, CA 92037

J. Ross
Department of Chemistry
Stanford University
Stanford, CA 94305

R. Sawyer
Department of Mechanical Engineering
University of California
Berkeley, CA 94720

W. P. Slichter
Executive Director
Research-Materials Science
and Engineering Division
Bell Laboratories
600 Mountain Avenue
Murray Hill, NJ 07974

O. W. Adams
Fundamental Interactions Branch, ER-161
Division of Chemical Sciences
Office of Basic Energy Sciences
U.S. Department of Energy
Mail Station J-309, GTN
Washington, D.C. 20545

J. W. Birkeland
Division of Power Systems
U.S. Department of Energy
Washington, D.C. 20545

L. C. Ianniello, Chief
Metallurgy and Ceramics Branch
Office of Basic Energy Sciences
U.S. Department of Energy
Washington, D.C. 20545

R. J. Kandel, Chief
Fundamental Interactions Branch, ER-161
Division of Chemical Sciences
Office of Basic Energy Sciences
U.S. Department of Energy
Mail Station J-309, GTN
Washington, D.C. 20545

J. S. Kane
Associate Director for Basic Energy Sciences
Office of Energy Research
U.S. Department of Energy
Washington, D.C. 20545

E. S. Pierce, Director
Division of Chemical Sciences, ER-16
Office of Basic Energy Sciences
U.S. Department of Energy
Mail Station J-309, GTN
Washington, D.C. 20545

M. C. Wittels, Chief
Solid-State Physics and Materials
Chemistry Branch
Office of Basic Energy Sciences
U.S. Department of Energy
Washington, D.C. 20545

A. Narath, 4000
J. B. Gerardo, 4210
J. K. Galt, 5000
T. B. Cook, 8000; Attn: L. Gutierrez, 8400
W. J. Spencer, 8100
A. N. Blackwell, 8200
B. F. Murphey, 8300
D. M. Schuster, 8310
R. L. Rinne, 8320
G. W. Anderson, 8330
W. Bauer, 8340
P. L. Mattern, 8342
D. L. Hartley, 8350
M. A. Gusinow, 8351 (10)
C. W. Robinson, 8352
D. R. Hardesty, 8353
B. R. Sanders, 8354
Division 8265 for TIC (27)
P. Dean - 8265/Technical Library Processes Division, 3141
Technical Library Processing Division, 3141 (2)
Library and Security Classification Division, 8266-2 (3)